BL2B

Velocity Map Imaging of Fragment Mixtures from Fullerenes

H. Katayanagi[1, 2] and K. Mitsuke[3]

[1]*Department of Photo-Molecular Science, Institute for Molecular Science, Okazaki 444-8585, Japan*

[2]*School of Physical Sciences, The Graduate University for Advanced Studies (SOKENDAI), Okazaki 444-8585, Japan*

[3]*Faculty of Science, Josai University, Sakado 350-0295, Japan*

We have developed a photofragment imaging spectrometer suitable for synchrotron radiation excitation of gaseous molecules of refractory materials such as fullerenes [1, 2]. Using this imaging spectrometer we have measured "*yt* images" in which fragment masses are shown in *t* axis and one-dimensional velocity distributions of the fragments are shown in *y* axis. Translational temperatures (T_{trans}) of the fragments were obtained from the *y* distributions of the fragments. Values of average kinetic energy release were obtained from T_{trans}.

So far the velocity map images (*xy* images) have been used to elucidate photodissociation mechanisms of small molecules [3]. Prodhan et al. have expected that velocity map images of fullerene fragments would reveal details of photodissociation mechanism of the fullerenes [4]. Thus we tried to obtain *xy* images of fragments from the fullerenes in the present study.

The experiments were performed at BL2B in UVSOR. Fullerene powder was loaded in a quartz tube and heated up by an electric heater in vacuum. The fullerene vapor passed through two apertures and reached the ionization region. The fullerene molecular beam thus generated along *x* axis intersected the monochromatized synchrotron radiation (*y* axis) at the ionization region. Ions produced there were extracted by a velocity map imaging electrode assembly and projected along *z* axis on to a position sensitive detector (PSD). Hence the *xy* images were obtained on the PSD.

Figure 1(a) shows the experimental *xy* image of parent ions (C_{70}^{2+}) in the molecular beam of C_{70} and 1(b) shows the *xy* image of a fragment mixture of C_{68}^{2+} - C_{58}^{2+} from C_{70} at the photon energy of 105 eV. Scattering velocity distributions of the fragments are expected to be isotropic [1], so that the fragment images should be circular. However Fig. 1(b) has an oval shape. This shape can be explained as the convolution of the isotropic velocity distribution of the fragments and the anisotropic velocity distribution of the parent molecular beam. These *xy* images have already been reported in Ref. 2.

Figure 2(a) shows the mixture of C_{58}^{2+} - C_{48}^{2+} fragments produced from C_{60} at the photon energy of 102 eV. The oval shape was observed. Figure 2(b) shows a result of computer simulation for C_{58}^{2+} fragments. In this simulation we assumed that the fragments were emitted isotropically with T_{trans} of 100 K from the anisotropic parent molecular beam of 685 K. Figure 2(b) is similar to 2(a), although 2(a) is a mixture of the fragments. This similarity suggests that the C_{58}^{2+} is the most abundant fragment and that all the fragments have velocity distributions following the Maxwell-Boltzmann distribution. These are in accord with the results in Refs. 1 and 2. However we cannot distinguish singularities of the velocity distributions for production of magic number fragments (C_{50}^{2+} from C_{60} [1] and C_{60}^{2+} from C_{70} [2]) on these *xy* images, because abundance of these magic number fragments are very small in the mixtures.

We are trying to obtain the *xy* images of such scarce fragments with improvement of our imaging spectrometer. Observing such *xy* images will allow us to examine finer details of the production mechanisms of the magic number fragments. This will lead to the understanding of the formation mechanism of the fullerenes.

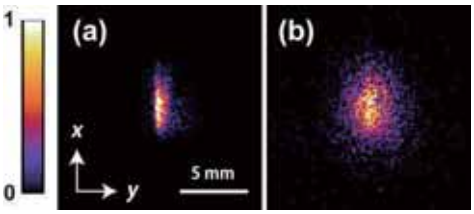

Fig. 1. Velocity map (*xy*) images of (a) parent molecular beam and (b) fragment mixtures from C_{70}.

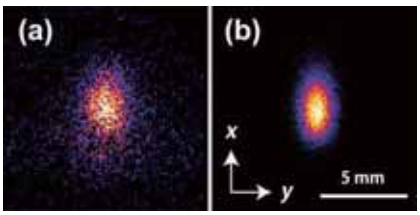

Fig. 2. Velocity map (*xy*) images of (a) fragment mixtures from C_{60} and (b) simulated image of C_{58}^{2+} fragments.

[1] H. Katayanagi and K. Mitsuke, J. Chem. Phys. **133** (2010) 081101.

[2] H. Katayanagi and K. Mitsuke, J. Chem. Phys. **135** (2011) 144307.

[3] A. T. J. B. Eppink and D. H. Parker, Rev. Sci. Instrum. **68** (1997) 3477.

[4] Md. S. I. Prodhan *et al.*, Chem. Phys. Lett. **469** (2009) 19.

BL3U

Electrochemical Reaction Studied by Soft X-Ray Absorption Spectroscopy I. Development of Liquid Cell for Electrochemistry

M. Nagasaka[1], H. Yuzawa[1], T. Horigome[1], A. P. Hitchcock[2] and N. Kosugi[1]
[1]*Institute for Molecular Science, Myodaiji, Okazaki 444-8585, Japan*
[2]*Department of Chemistry, McMaster University, Hamilton, ON L8S 4M1, Canada*

To better understanding electrochemistry, it is necessary to investigate the structures of electrolytes including electric double layers at different potentials. The structures of electric double layers were mainly studied by vibrational spectroscopies as reviewed by Ashley and Pons [1], in which the structures of solvent water molecules were determined from the OH stretching mode. It is difficult to investigate the structures of electrolytic solutes in dilute electrolyte solutions. Soft X-ray absorption spectroscopy (XAS) is a powerful tool to study local electronic structure of liquids. The structures of solutes are observed element-selectively even in dilute solutions. Recently, we have developed a liquid cell for the measurement of XAS in transmission mode [2]. In this work, we have developed an in-situ XAS measurement system for studying electrochemical reactions of electrolytes by using the liquid cell with built-in electrodes.

The experiments were performed at BL3U. Figure 1(a) shows schematics of the liquid cell. It consists of four regions I, II, III, and IV, separated by 100 nm-thick Si_3N_4 membranes (NTT AT Co.). Region I is connected to the beam line under vacuum. Regions II and IV are at atmospheric pressure of helium gas. The flow rate of helium gas is controlled by a mass flow controller, and the helium pressure is adjusted by a needle valve set in the gas outlet. The thin liquid layer (region III) is sandwiched between two Si_3N_4 membranes with spacers. Liquid samples are substituted by other samples in combination with a tubing pumping system. The thickness of the liquid layer can be varied from 20 to 2000 nm by changing the He backpressure in regions II and IV [2]. Soft X-rays, which pass through region II and the liquid layer III, are detected by a photodiode (IRD AXUV100) in region IV.

For the investigation of electrochemical reactions, three electrodes are included in the liquid layer III, as shown in Fig. 1(b). The working electrode (WE) is a Au deposited Si_3N_4 membrane, which is one side of the liquid layer III. This membrane is connected with a Au tab for electric conduction. At the opposite side of the Au contact is a teflon™ spacer. The counter electrode (CE) is a Pt mesh. The reference electrode (RE) is a Ag/AgCl electrode with saturated KCl solution, which is isolated from liquid samples by a teflon™ cover. The potential is controlled using a potentiostat (Solartron 1287).

In the present configuration, XAS spectra of electrolytes can be measured at different potentials by using this system. The XAS spectra of solutes in dilute electrolyte solutions are obtained by adjusting the thickness of the liquid layer. We have investigated the change in valence of Fe ions in aqueous iron sulfate solutions by measuring Fe L-edge XAS at different potentials. These results are discussed elsewhere in this volume [3].

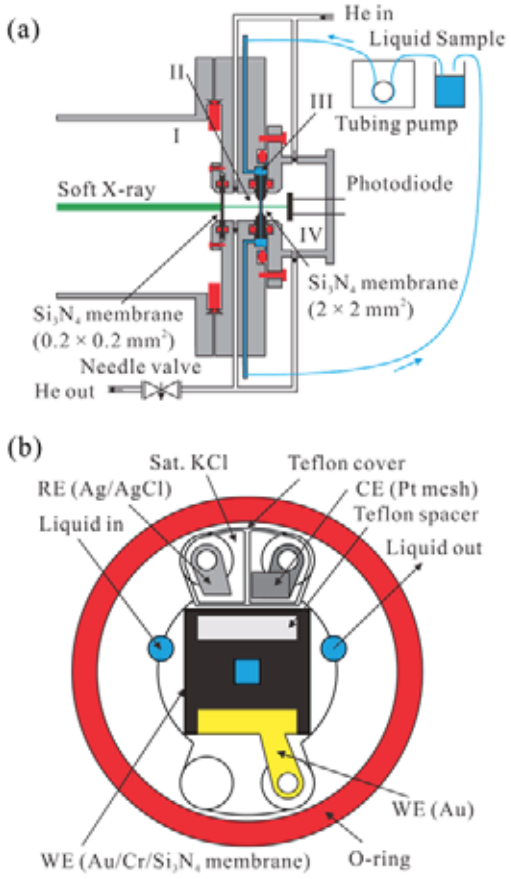

Fig. 1. (a) Schematic of the liquid cell for XAS in transmission mode. (b) Schematics of three electrodes included in the liquid cell.

[1] K. Ashley and S. Pons, Chem. Rev. **88** (1988) 673.
[2] M. Nagasaka *et al.*, J. Electron Spectrosc. Relat. Phenom. **177** (2010) 130.
[3] M. Nagasaka *et al.*, in this volume.

BL3U

Electrochemical Reaction Studied by Soft X-Ray Absorption Spectroscopy II. Valence Changes of Fe Ions in Aqueous Iron Sulfate Solutions

M. Nagasaka[1], H. Yuzawa[1], T. Horigome[1], A. P. Hitchcock[2] and N. Kosugi[1]
[1]*Institute for Molecular Science, Myodaiji, Okazaki 444-8585, Japan*
[2]*Department of Chemistry, McMaster University, Hamilton, ON L8S 4M1, Canada*

The redox reactions of Fe ions are one of the most common electrochemical systems because of their importance in a variety of fields. Previously, Fe redox reactions were mainly studied by voltammetric methods [1], but it is difficult to measure the change in valence of Fe ions in dilute electrolyte solutions. Soft X-ray absorption spectroscopy (XAS) is a powerful tool to study local electronic structures of liquids. Recently, we have developed a liquid cell for XAS in transmission mode [2]. We have also developed an in-situ system for electrochemistry by using the liquid cell with built-in electrodes [3]. Here we report Fe L-edge XAS results for the change in valence of Fe ions in an aqueous iron sulfate solution induced by variation of the potential at a gold electrode. The experiments were performed at BL3U. The details of the liquid cell are described in this volume [3]. The electrolyte is 0.5 M aqueous iron sulfate at pH = 2.2.

Figure 1 shows the Fe L-edge XAS spectra of an aqueous iron sulfate solution at different potentials. Each XAS spectrum is measured at a constant potential. The XAS L_3 spectra have signals from Fe(II) and Fe(III) ions and show an isosbestic point, indicating only two species are involved. As shown in Fig. 1(a), a nonlinear oxidation of Fe(II) to Fe(III) ions is observed when the potential is increased from 0.0 to 0.9 V. On the other hand, the reduction of Fe(III) to Fe(II) ions varies linearly with the potential when the potential is decreased from 0.9 to -0.4 V, as shown in Fig. 1(b).

Figure 2 shows the fraction of Fe(II) ions from total Fe ions at different potentials, which is determined from the curve fitting procedure of the XAS spectra. The amount of Fe(II) ions decreases by oxidation of Fe(II) to Fe(III) with increasing the potential. Two oxidation processes are revealed. One is a simple oxidation process and the other is a process involving the sulfate ions, which affect electrode kinetic parameters and diffusion coefficients [1]. On the other hand, the formation of Fe(II) from Fe(III) with decreasing the potential is a simple reduction of Fe(III) ions. We will investigate these redox processes by correlating with the XAS results from the cyclic voltammetry at different scanning rates.

[1] A. F. Gil *et al.*, J. Electroanal. Chem. **417** (1996) 129.
[2] M. Nagasaka *et al.*, J. Electron Spectrosc. Relat. Phenom. **177** (2010) 130.
[3] M. Nagasaka *et al.*, in this volume.

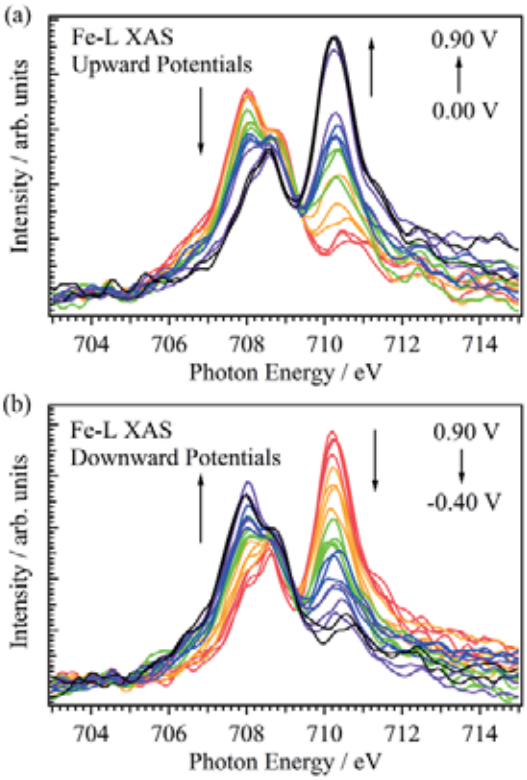

Fig. 1. Fe L-edge XAS spectra of Fe ions in a 0.5 M aqueous iron sulfate solution at different potentials; (a) increasing from 0.00 to 0.90 V, and (b) decreasing from 0.90 to -0.40 V.

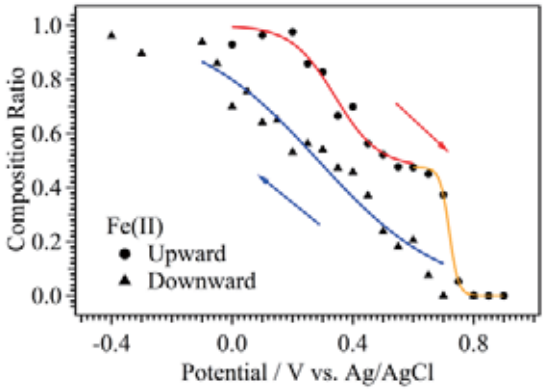

Fig. 2. Fractional composition of Fe(II) ions as a function of potential, obtained from Fe L-edge XAS spectra measured at different potentials.

In-Situ Observation of Solid-Liquid Heterogeneous Catalytic Reaction by Soft X-ray Absorption Spectroscopy

H. Yuzawa, M. Nagasaka and N. Kosugi
Institute for Molecular Science, Myodaiji, Okazaki 444-8585, Japan

Study of catalytic reaction mechanism is important to obtain some clue to the improvement of activity and selectivity. In-situ observation of the catalytic reaction by spectroscopic approaches such as FT-IR, NMR and XPS, are effective methods to elucidate the reaction mechanism. However, in-situ observation of solid-liquid heterogeneous catalytic reaction is difficult because the photoabsorption of bulk liquids (substrate and/or solvent) hinder the objective change in the spectrum. The spectroscopic observation of this kind of system has been generally carried out by using vapor substrate adsorbed on the catalyst surface instead of liquid substrate [1] although its condition is different from the real one.

We developed a transmission-type liquid cell, which is able to control easily the liquid thin layer, for the soft X-ray XAS [2] and demonstrated that this spectroscopic method was effective to clarify the local structure of various liquid solutions [3]. Thus, in this study, we have extended this method to the in-situ observation of solid-liquid heterogeneous catalytic reaction. As a probe reaction, we have selected hydration of cyanopyrazine on TiO_2 (eq. 1).

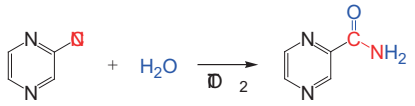

(1)

The experiments were carried out in BL3U. Suspension of catalyst was prepared by mixing of cyanopyrazine (3 ml, 0.78 M), ethanol (5 ml), water (35 ml) and TiO_2 (JRC-TIO-4, 0.15 g). Then, the suspension of thin layer (< 1 μm thickness) was sandwiched between two 100 nm-thick Si_3N_4 membranes, and the C K-edge XAS was measured at 323.8−338.5 K. The photon energy was calibrated by the C 1s−3pt$_2$ Rydberg peak (297.99 eV) of the CH_4 gas mixture in He [4].

Figure 1a shows the C K-edge XAS spectra of cyanopyrazine, pyrazinamide at 298K and hydration of cyanopyrazine at 331.5 K. Three absorption peaks (285.4, 286.0 and 286.6 eV) are observed in cyanopyrazine (red line) and one absorption peak (285.3 eV) is observed in pyrazinamide (blue line). All these peaks are assigned to the 1s−π* excitation. Other absorption peaks could not be observed in the higher photon energy than 287 eV because of overlap with the C K-edge absorption of ethanol. In the spectra of cyanopyrazine hydration (green lines), the intensity of the absorption peak at 285.4 eV decreases slightly, while the other two peaks decrease conspicuously with the reaction time, corresponding to the production of pyrazinamide. Figure 1b shows a logarithmic plot for the normalized XAS intensity of cyanopyrazine, which is obtained from the factor analysis for Figure 1a (green lines) by using the standard spectra of cyanopyrazine and pyrazinamide. This plot shows linear relationship to the reaction time, indicating that the observed catalytic reaction is the first-order reaction for the concentration of cyanopyrazine and the slope of the line is a reaction rate constant. When the same procedure is applied to the hydration reaction in other temperatures (325.1, 329.8 and 338.5 K), the linear relationship is also obtained. The obtained rate constants show linear relationship in the Arrhenius plot (E_a = 52.4 kJ/mol). Thus, this analytical procedure would be reasonable.

Through the above experiments, we can conclude that the transmission soft X-ray XAS approach has a potential for the in-situ observation of the solid-liquid heterogeneous catalysis. In the future, we will improve the system to observe reaction intermediates.

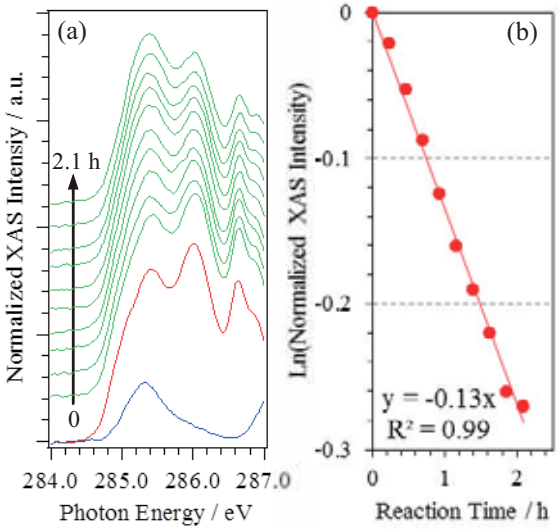

Fig. 1. (a) C K-edge XAS spectra for the cyanopyrazine (0.78 M)−ethanol−water solution (red line), pyrazinamide (0.20 M)−ethanol−water solution (blue line) at 298 K and catalytic hydration of cyanopyrazine on TiO_2 (10 scans (0−2.1 h), green lines) at 331.5 K. (b) A logarithmic plot of the normalized XAS intensity of cyanopyrazine obtained from the factor analysis of green lines in (a).

[1] A. Vimont *et al.*, Chem. Soc. Rev. **39** (2010) 4928.
[2] M. Nagasaka *et al.*, J. Electron Spectrosc. Relat. Phenom. **177** (2010) 130.
[3] For example, M. Nagasaka *et al.*, UVSOR Activity Report **37** (2010) 57.
[4] K. Ueda *et al.*, Chem. Phys. Lett. **236** (1995) 311.

BL4B

Development of a High-Resolution Magnetic Bottle Electron Spectrometer

M. Sawa[1], Y. Konosu[1], K. Soejima[1], E. Shigemasa[2] and Y. Hikosaka[1]

[1]*Department of Environmental Science, Niigata University, Niigata 950-2181, Japan*

[2]*UVSOR Facility, Institute for Molecular Science, Okazaki 444-8585, Japan*

Observing kinetic energy correlation for all the emitted electrons is very useful to understand multiple ionization process of molecules. Such multi-electron coincidence measurements can be achieved with an electron spectrometer using magnetic bottle technique. However, it is difficult for a magnetic bottle electron spectrometer to observe high energy electrons with sufficient energy resolutions, because of their short time-of-flights (TOFs). We have introduced retarding electrodes into our magnetic bottle electron spectrometer, in order to improve energy resolution for high energy electrons.

The electron retarding system consists of an inner drift tube and three metal meshes, as schematically illustrated in Fig. 1. Electrons collected by an inhomogeneous magnetic field in the ionization region are retarded between first and second meshes, when we apply a negative voltage to the second mesh and the inside drift tube. This retardation expands electron TOFs, and higher energy resolution can be achieved.

We have carried out photoelectron-Auger electron coincidence measurements with the electron retarding system to evaluate the kinetic energy resolution and detection efficiency. The results are shown in Fig. 2. Compared to the original energy resolution of $E/\Delta E$ = 35 (black dots), the energy resolution is improved up to $E/\Delta E > 200$ by applying retardation voltages. Here, while we cannot observe electrons with lower energies than the retardation voltages, and we has to adjust the retardation voltage to a value lower than the energies of the concerned electrons. The bottom panel of Fig. 2 shows detection efficiencies determined by the ratios between all photoelectron yields and the photoelectron yields measured in coincidence with Auger electron. The detection efficiencies are fairly constant against electron energy, even when the retarding voltage of -180 or -320 V is applied. The detection efficiencies around 50% are reasonable considering the transmission efficiencies of the three meshes and the detection efficiency of the microchannel detector.

We have applied the developed system to the observation of the OCS S2p photoionization and the subsequent Auger decay. Figure 3 displays a two-dimensional map of the coincidence yields between the S2p photoelectron and Auger electrons. The spin-orbit splitting of the $S2p^{-1}$ state is resolved (see the right panel), and the Auger spectrum associated with each core-hole state is derived (the top panel). From these coincidence spectra, the Auger transition probabilities from the two core-hole states can be evaluated.

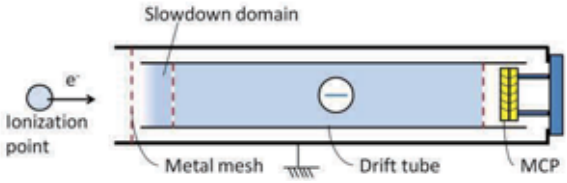

Fig. 1. Schematic of the electron retarding system.

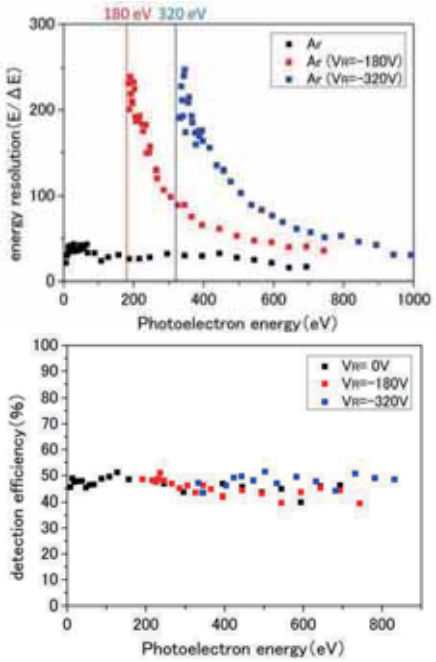

Fig. 2. Energy resolutions (a) and Detection efficiencies (b) observed with/without retarding voltages.

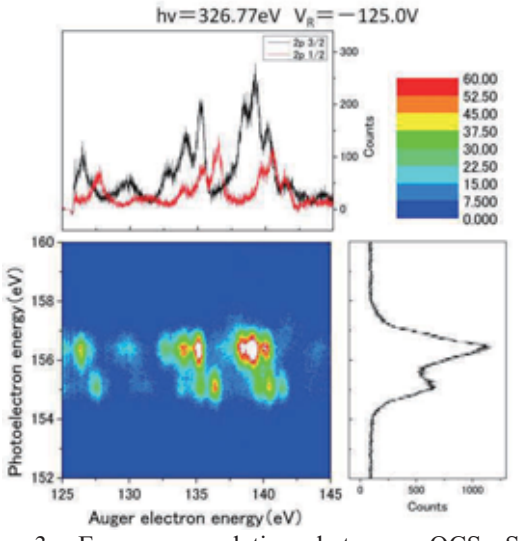

Fig. 3. Energy correlation between OCS S2p photoelectrons and Auger electrons.

Development of a Novel Pulsed Nozzle for Probing Large Molecules in Vacuum Chamber

T. Tajiri, K. Sakamoto, T. Gejo and K. Honma
Univ. of Hyogo, Koto 3-2-1, Kamigori-cho, Hyogo 678-1205, Japan

The liquid water has been regarded as fundamental material and has been investigated for many years. Particularly interest is the hydrogen network in liquid water, which were investigated by many spectroscopic studies. Since then, many models have been proposed. Recently, in order to investigate the electronic states of liquid water with hydrogen networks, photoelectron spectroscopy and soft x-ray emission spectra have been investigated. To obtain those spectra, liquid phase in vacuum chamber is necessary. Therefore, liquid water beam technique has been employed.

For this liquid phase experiments, we have developed the device that utilizes ultrasonic atomization to produce a dense aerosol microdroplet of water. The ultrasonic atomization technique has been used for generate the microdroplets in mist: The size of liquid droplets was distributed around the micrometer scale. Therefore one can achieve micro droplet of liquid water in vacuum chamber by the injecting them directly.

Last year we have utilized a nozzle with a aperture of 500 μm diameter. Although we have tried to measure photoelectron spectra with this nozzle, low intensity did not allow any significant measurement. This time, we modified the nozzle, in which pulsed valve with high conductance is used.

The experiments were carried out on the bending beamline BL5B at the UVSOR facility in IMS. As figure 1 shows, the experimental set-up consists of three parts: a mist generation part, a transportation part and a nozzle. The microdroplets are generated via ultrasonic atomization. Ultrasonic oscillators (HM2412, Honda Electronics Co., Ltd) operating at 2.4 MHz were installed at the bottom of the water bath. The microdroplet were carried by He and pumped out to obtain a stable stream. A pulsed valve has been placed just before pumping system and the generated microdroplet going into the vacuum chamber. After 10 mm down stream, 10 - 15 eV VUV photons have been radiated to the microdroplets and the excitation UV fluorescence spectra has been measured by photomultiplier tube (R928, HAMAMATSU) installed.

Figure 2 shows the cross section of the pulsed nozzle for microdoloplet. We have modified commercially available General Valve Series 9 with its magnetically activated plunger, which is widely used in the field of atomic and molecular beams. These types produce pulses with a typical width of a few hundreds of microseconds. The 45-mm long, 1.5 mm in diameter plunger was attached to the armature and operated with a repetition rate in the 1–2 Hz range.

The time profile shows the large molecular are generated relatively slowly after opening the nozzle. Main signal due to mist arises 5 ms after the opening. Since the fluorescence excitation spectra of water clusters strongly depend on its cluster size [1], we can estimate the mean size of droplet in vacuum chamber by these spectra. Simple analysis shows that the size is more than 1000.

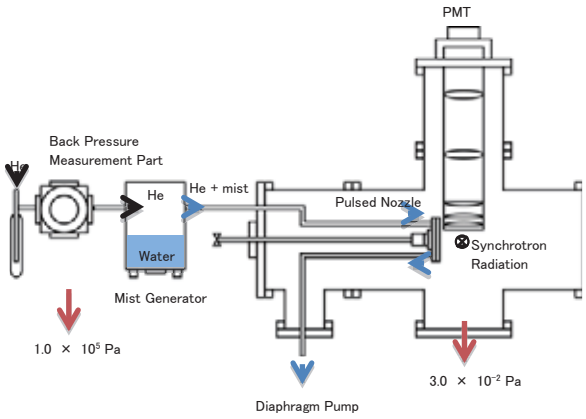

Fig. 1. The experimental set-up for the microdroplet generation in vacuum chamber.

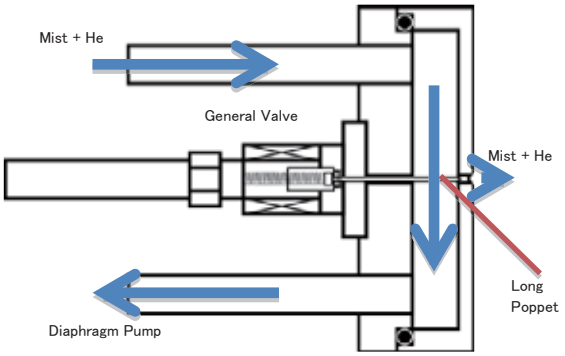

Fig. 2. The cross section view of the pulsed nozzle for microdroplet.

[1] M. Ahmed *et al.*, J. Phys. Chem. A **98** (1994) 12530.

BL5B, BL7B

Applicability of Database Values of Atomic Mass Absorption Coefficients on Absorption Spectra of L-alanyl-L-alanine Film from 3 to 250 eV

Y. Tanigawa[1], Y. Momoki[1], K. Ishiyama[2], S. Takenaka[2] and K. Nakagawa[1, 2]

[1]*Graguate school of Human Development and Environment, Kobe University, Kobe 657-8501, Japan*

[2]*Faculty of Human Development, Kobe University, Kobe 657-8501, Japan*

Absorption spectra of thin films of L-alanyl-L-alanine $C_6H_{12}N_2O_3$ were measured at the photon energy from 3 eV to 250 eV in an attempt to discuss with which energy of radiation is responsible for chemical evolution in space where molecules interact with electromagnetic radiation with wide energy range [1].

Powder of L-alanyl-L-alanine was purchased from SIGMA Pharmacy Company. We prepared thin films of L-alanyl-L-alanine with the vacuum evaporation technique in which heater temperature was set at about 370 K. Collodion films or SiO_2 plates were used as substrate. Prepared thin films were transferred to the measurement system without any contact with air.

Spectral measurement was carried out at the beamlines 5B and 7B. Photon energy region used for measurements were 3.5 to 37 eV at BL7B and 30 to 250 eV at BL5B. Optical density $OD(E)$ was obtained as a function of photon energy E for various samples with different thickness because magnitude of $OD(E)$ around 20 eV was one order larger than that around 90 eV or at higher energies. Here $OD(E)$ was determined to be $OD(E) = \log(I_0(E)/I(E))$, where $I_0(E)$ and $I(E)$ are transmitted light intensity of (substrate) and that of (substrate+sample). Different spectra obtained for different sample were connected. Finally we obtained a smooth spectrum. Similar result was already reported by our group [2].

Translation from $OD(E)$ to absorption cross section $\sigma(E)$ was carried out using following equations;

$$I(E) = I_0(E)e^{-\sigma(E)nl}, \qquad (1)$$

and

$$nSl = N_{\mathrm{HPL}} . \qquad (2)$$

Equation (1) is the Lambert-Beer law, where n the number density of sample and l the pass length. The left side of equation (2) shows the total number of L-alanyl-L-alanine molecules in a film of which area is S and the right side shows the total number of L-alanyl-L-alanine molecules in a film analyzed by a high performance liquid chromatography (HPLC).

The first step of our translation from $OD(E)$ to $\sigma(E)$ was carried out around 7 eV for films evaporated on SiO_2 substrate. We cannot use this technique for the films on the collodion substrate because collodion might damage the HPLC system.

Figure 1 shows the absolute values of absorption spectra of L-alanyl-L-alanine film. Vertical axis of the figure was again translated into the optical oscillator strength distribution df/dE determined by the relation [3];

$$\frac{df}{dE}(\mathrm{eV}^{-1}) = 1.80 \times \sum_{\mathrm{q}} \chi_{\mathrm{q}} \mu_{\mathrm{aq}}(\mathrm{Mb}) , \qquad (3)$$

In the equation 3, χ_q is the number of atom q in that molecule and μ_{aq} is the atomic absorption coefficient of atom q in the unit of Mb.

In Fig. 1, the curve A is df/dE spectrum obtained in this work and the curve B shows the calculated result by eq. (3) using the atomic absorption coefficient by Henke et al. [4].

As seen from the figure, curve B can reasonably reproduce the experimental result (curve A). In order to check the applicability in detail of the Henke's atomic absorption coefficient to our L-alanyl-L-alanine data, we extrapolated 250-280 eV part to the region of E >280 eV to obtain the curve C. Making the integration of spectrum from 5 eV to 10000 eV along with the curve C, we obtained value of 62.7 which is very close to 64, the number of 2s and 2p electrons in L-alanyl-L-alanine molecule. Thus we concluded that the Henke's atomic absorption coefficient can reproduce the absorption spectrum within the region from 30eV to 200eV.

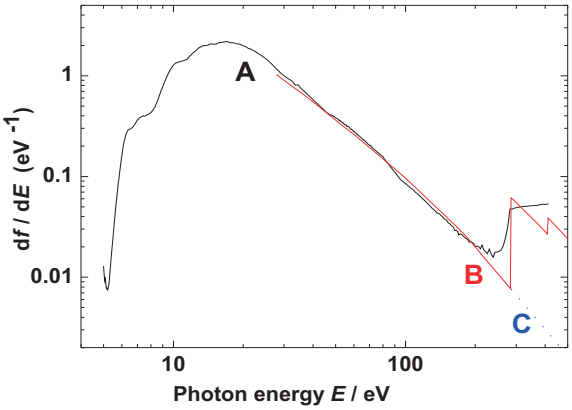

Fig. 1. Absorption spectrum of L-alanyl-l-alanine film. Curve A: Result in this Work. Curve B: Calculated result with Henke [4]. Curve c: See text.

[1]K. Nakagawa, Viva Origino, 37 (2009) 24, in Japanese.

[2] M. Kamohara *et al.,* Rad. Phys. Chem. **77** (2008) 1153.

[3] Y. Hatano, In: Sham, T.K. (Ed.), Chemical Applications of Synchrotron Radiation Part I. World Scientific, Singapore, (2002) 55.

[4] B. L. Henke *et al.,* Atomic Data and Nuclear Data Tables, **54**(1993)181.

BL6U

Site-Specific Fragmentation Driven by Particular Auger Processes of the C K-Shell Excited *cis*-Hexafluorocyclobutane Molecule

S. Ishikawa[1], K. Okada[1], H. Iwayama[2,3], L. Ishikawa[2] and E. Shigemasa[2,3]

[1]*Department of Chemistry, Hiroshima University, Higashi-Hiroshima 739-8526, Japan*

[2]*UVSOR Facility, Institute for Molecular Science, Okazaki 444-8585, Japan*

[3]*School of Physical Sciences, Graduate University for Advanced Studies (SOKENDAI), Okazaki 444-8585, Japan*

Inner-shell excited states of molecules relax into various molecular cationic states through Auger decays. The resultant cations are in general unstable and dissociate into fragment ions. Information on the correlation between the Auger-final states and the products provides us deeper insight into the fragmentation dynamics of the inner-shell excited molecules. We found in our previous study that after the $C1s^{-1}\sigma_{CC}^*$ and $F1s^{-1}\sigma_{CC}^*$ transitions the *cis*-1,1,2,2,3,4- hexafluorocyclobutane (*cis*-c-$C_4H_2F_6$) molecule dissociates into the fragment ions with C–F bond(s) in higher yield. In this study we have acquired the Auger-electron–photoion coincidence data of the *cis*-c-$C_4H_2F_6$ molecule at the C 1s edge by using a pair of a double toroidal electron analyzer (DTA) and an ion time-of-flight mass spectrometer to obtain information on the Auger processes correlating with such specific fragments.

The experiments have been performed on the soft X-ray beamline BL6U. The experimental setup has been described in a previous paper [1]. Synchrotron radiation was irradiated at right angles to the effusive beam of the gaseous *cis*-c-$C_4H_2F_6$ sample. The electrons traveling through the DTA tube were detected with a position sensitive detector (RoentDek, DLD40). Fragment ions were extracted toward the time-of-flight spectrometer by a pulsed electric field applied just after the Auger electron detection across the ionization region. The coincidence data were obtained as list-mode files, containing a series of a set of the detected electron positions and the ion arrival times. They were acquired in this study at the photon energies of 290.3, 292.8, 297.0 and 327.6 eV.

The resonant Auger spectrum obtained at the photon energy of 297.0 eV has characteristic features that distinguish it from the other spectra acquired in this study. Figure 1a shows the resonant Auger spectrum measured at 297.0 eV and the components coincident with the $CH_{0,1}F^+$, $CH_{0,1}F_2^+$ and $C_2H_{0,1}F_3^+$ fragments. The excitation energy corresponds to the $\sigma_{CC}^* \leftarrow C_{CF2}$ 1s transition of *cis*-c-$C_4H_2F_6$, where C_{CF2} means the carbon of a CF_2 group. The spectra taken at 292.8 eV are also displayed in Fig. 1b for comparison. The intense peak at the final-state energy around 42 eV is distinctive of the 297.0-eV excitation. The coincidence spectra reveal that in this peak the $CH_{0,1}F^+$ and $CH_{0,1}F_2^+$ ions are produced in abundance, whereas the spectra of the fragment ions without a C–F bond give no peak (not shown in Fig. 1). We can conclude that the Auger-final states corresponding to this energy region are responsible for the production of the specific fragment ions. This study clearly demonstrates that the site-specific fragmentation of the C K-shell excited *cis*-c-$C_4H_2F_6$ molecule is strongly correlated with the particular Auger decays.

The experiments at the F K-edge are eagerly in progress and the results will be published in the near future.

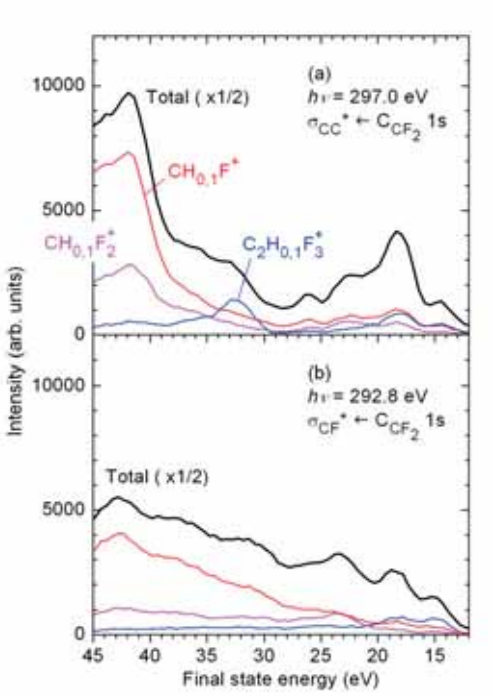

Fig. 1. Resonant Auger spectra coincident with the $CH_{0,1}F^+$, $CH_{0,1}F_2^+$ and $C_2H_{0,1}F_3^+$ fragments acquired at 297.0 eV (panel a) and 292.8 eV (panel b). Total resonant Auger spectra are also plotted as the thicker black lines and are scaled by a half. Abscissa has been obtained as the difference between the photon energy and the electron kinetic energy.

[1] T. Kaneyasu, Y. Hikosaka and E. Shigemasa, J. Electron Spectrosc. Relat. Phenom. **156-158** (2007) 279.

BL6U

Formation of Metastable Carbon Dioxide Dications Following Core-Hole Creation

Y. Shibata[1], K. Soejima[1], H. Iwayama[2], E. Shigemasa[2] and Y. Hikosaka[1]
[1]*Department of Environmental Science, Niigata University, Niigata 950-2181, Japan*
[2]*UVSOR Facility, Institute for Molecular Science, Okazaki 444-8585, Japan*

The ion yield spectra observed in the inner-shell threshold ranges of carbon dioxide (CO_2) molecules [1] indicate that metastable CO_2^{2+} is favorably produced in the Auger decay of the O 1s core-hole state, compared to the Auger decay of the C1s core-hole state. In this study, we have used an Auger-electron-ion coincidence method to investigate the formation mechanism of the metastable dications following the core-hole creations in CO_2.

The experiment was performed at the undulator beamline BL6U, using an electron-ion coincidence spectrometer [2]. The electrons were analyzed in energy by a double toroidal electron analyzer, while ions were extracted from the interaction region into an ion momentum spectrometer by a pulsed electric field according to the detection of the electron.

Figure 1(a) shows an O 1s Auger spectrum of CO_2, plotted as a function of the kinetic energy and of the binding energy. The Auger spectrum exhibits several band structures corresponding to the formation of different CO_2^{2+} states. Figures 1(b), (c) and (d) represent the spectra of Auger electrons observed in coincidences with metastable CO_2^{2+}, O^++CO^+ ion pairs and C^++O^+ ion pairs, respectively. One finds that the formation of metastable CO_2^{2+} is associated with the Auger decay into doubly charged states in the binding energy range of 35-45eV. A calculation implies that the doubly charged states have the electronic configuration of π^{-2} [3].

Figure 2 compares the Auger spectra observed in the decays of the O1s and C1s core-holes, where the red curves are obtained in coincidences with metastable CO_2^{2+}. While the CO_2^{2+} states in the same binding energy range are relevant to the metastable CO_2^{2+} formation following the different core-hole creations, the intensity of the metastable CO_2^{2+} formation is about four times more intense in the O 1s core-hole decay. The favorable production of metastable CO_2^{2+} following the O 1s core-hole creation is qualitatively explained by considering the spatial distribution of the π orbital involved in the decay processes. Since the π valence orbital is mostly localized around the O atom in the CO_2 molecule, the π electron preferentially fills the O 1s core-hole due to a large overlap between the core and valence orbitals. Thus the Auger transition involving the π electrons is favored in the decay of the O 1s core-hole states rather than the C core-hole states, resulting in the favorable formation of metastable CO_2^{2+} states with the configuration of π^{-2} in the decay of the O 1s core-hole states.

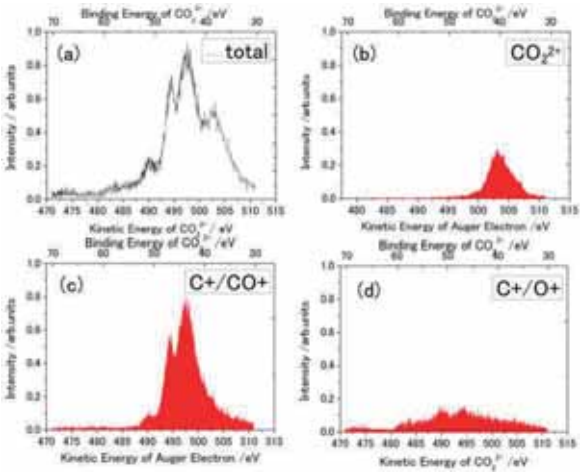

Fig. 1. O1s Auger spectrum (a) and Auger spectra obtained in coincidences with (b) metastable CO_2^{2+}, (c) O^++CO^+ ion pairs and (d) C^++O^+ ion pairs.

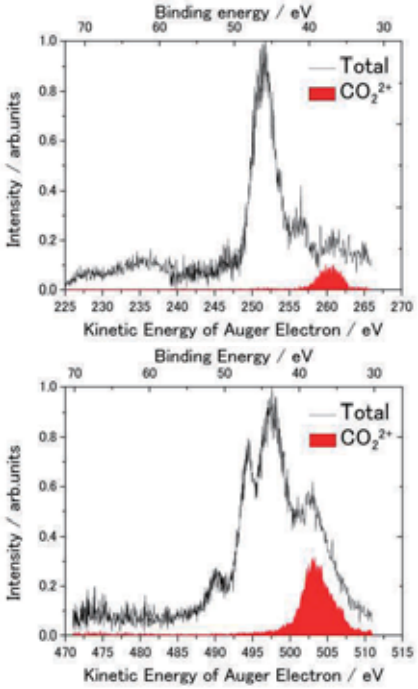

Fig. 2. O1s and C1s Auger spectra (solid lines) and Auger spectra (a) and Auger spectra obtained in coincidences with metastable CO_2^{2+} (red).

[1] G. Ohrwal *et al*., J. Phys. B **35** (2002) 4543.
[2] T. Kaneyasu *et al*., J. Electron Spectrosc. Relat. Phenom. **156-158** (2007) 279.
[3] J. A. Kelber *et al*., J. Chem. Phys. **75** (1981) 652.

High-Resolution Electron Spectroscopy for Ethyl Trifluoroacetate

H. Iwayama[1], F. Penent[2], P. Lablanquie[2] and E. Shigemasa[1]
[1]*UVSOR Facility, Institute for Molecular Science, Okazaki 444-8585, Japan*
[2]*LCPMR, Université Pierre et Marie Curie, 75231 Paris Cedex 05, France*

Inner-shell photoionization of light elements is mostly relaxed via an Auger decay process, causing the emission of another electron from an outer-shell. Auger electron spectroscopy (AES) is thus an element-sensitive method with various analytical applications. Since a core hole can be regarded as being strongly localized at a particular atom, it can be expected that the Auger final dicationic state has two valence holes which are also localized near the inner-shell ionized atom. According to this simple atomic picture, the binding energies of the molecular Auger final states would also show chemical shifts. Owing to a hole-hole repulsion, the chemical shift in Auger electron spectra reflects any localization character of the two valence holes.

The interpretation of molecular Auger spectra is complex and the difficulties increase with increasing the number of atoms in a molecule. The Auger spectra become much more complicated in the case where a molecule is composed of several atoms of the same element. While well-defined photoelectron peaks reflecting the chemical shifts can be observed in photoelectron spectra, direct observations of the corresponding chemical shifts in molecular Auger spectra are practically impossible without using a coincidence technique. In order to stabilize the interpretation on the site-specific Auger spectra obtained by such coincidence experiments, however, high-resolution Auger electron spectra as well as theoretical calculations are indispensable. We have carried out high-resolution electron spectroscopic measurements on ethyl trifluoroacetate ($C_4H_5F_3O_2$).

The experiment was performed on the soft X-ray beamline BL6U at UVSOR. The radiation from an undulator was monochromatized by a variable included angle varied line-spacing plane grazing monochromator. The monochromatized radiation was introduced into a cell with sample gases. Kinetic energies of the emitted electrons were measured by a hemispherical electron energy analyzer (MBS-A1) placed at a right angle with respect to the photon beam direction. The direction of the electric vector was set to be parallel to the axis of the electrostatic lens of the analyzer. The kinetic energy resolution of the analyzer was set to 20 meV.

Figure 1(a) and 1(b) show the C 1s photoelectron and Auger electron spectra of $C_4H_5F_3O_2$ at the photon energy of 330 eV, respectively. The chemical shifts are clearly observed in Fig. 1(a). The oxygen and fluorine Auger electron spectra are displayed in Fig. 2 (a) and (b), respectively. It is seen that the populations of the Auger final states strongly depend on which core electron is ionized. No fine structure is found in every Auger electron spectrum, in spite of the high-resolution.

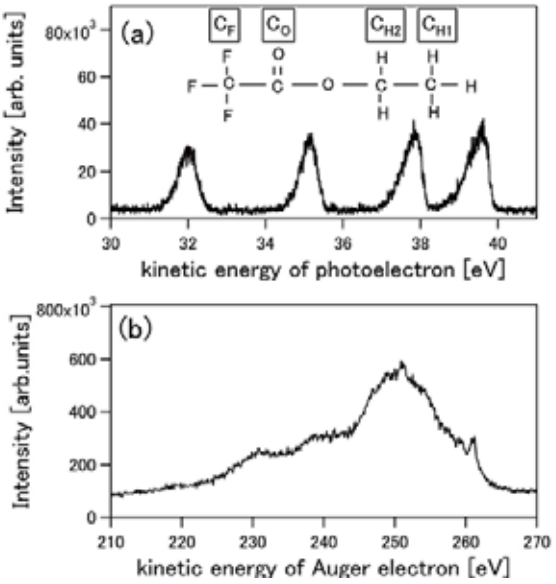

Fig. 1. (a) Carbon 1s photoelectron and (b) Auger electron spectra of $C_4H_5F_3O_2$.

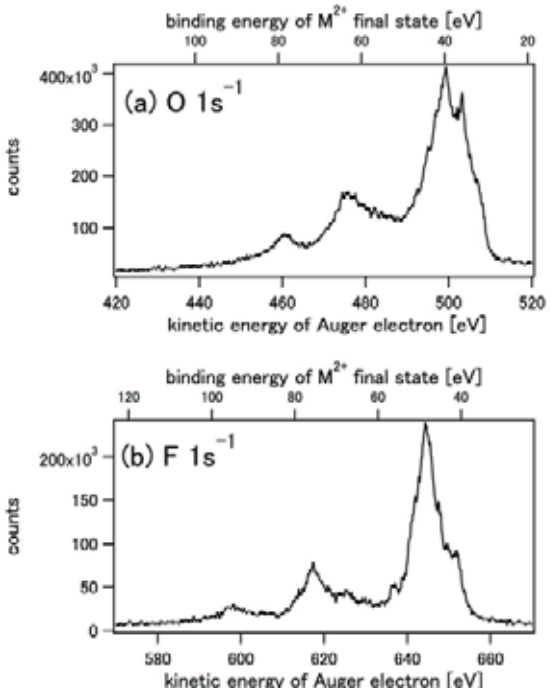

Fig. 2. (a) Oxygen and (b) fluorine Auger electron spectra of $C_4H_5F_3O_2$.

Deexcitation Processes after S 2p Photoexcitation of OCS Studied by Angle-Resolved Resonant Auger Electron Spectroscopy

L. Ishikawa, H. Iwayama and E. Shigemasa
UVSOR Facility, Institute for Molecular Science, Okazaki 444-8585, Japan

Soft X-ray absorption spectra of molecules exhibit rich structures in the region below the ionization thresholds, which are due to the excitations of a core electron to unoccupied valence or Rydberg orbitals. The core excited states are predominantly relaxed via Auger electron emission, in the case of the molecules composed of light elements, and subsequently fragmentation follows. Recent works on high-resolution resonant Auger electron spectroscopy have revealed that the nuclear motion of the molecular core-excited states is promoted in competition with the Auger decay.

In the previous work [1], three satellite structures (as labeled 0, 1, and 2 in Fig. 2) between B ($^2\Sigma$) and C ($^2\Sigma$) valence ionized states were observed following the S $2p_{3/2} \rightarrow \pi^*$ excitation, and they were assigned to $^4\Pi$, $^2\Pi$, and $^2\Phi$ shake-up-like states on the basis of ab initio theoretical calculations. Here, we revisit this first observation of spin-forbidden shake-up states. Angle-resolved two dimensional (2D) electron spectroscopy has been applied.

The experiments were carried out on the soft X-ray beamline BL6U. The radiation from an undulator was monochromatized by a variable included angle varied line-spacing plane grazing monochromator. For the 2D electron spectroscopy, the monochromator bandwidth was set to $E/\Delta E$ ~1000 at $h\nu$=165eV. Kinetic energies of the emitted electrons were measured by a hemispherical electron energy analyzer (MBS-A1) placed at a right angle relative to the photon beam direction. The direction of the electric vector was set to be either parallel (horizontal direction) or perpendicular (vertical direction) to the axis of the electrostatic lens of the analyzer. The resonant Auger spectra with kinetic energies ranging from 135 to 155 eV were recorded as a function of the photon energy in the S 2p excitation region.

Figure 1 shows the 2D maps of resonant Auger electron spectra following the S 2p excitation of OCS measured in horizontal (left) and vertical (right) directions. The horizontal solid lines in Fig. 1 indicate the resonance peak positions (S $2p_{3/2,1/2} \rightarrow \pi^*$ and S $2p_{3/2,1/2} \rightarrow \sigma^*$). The diagonal lines in Fig. 1 are due to the valence photoelectrons, while the vertical lines seen in the lower kinetic energy region are owing to the atomic Auger lines. The atomic line widths show clear polarization dependence, which may reflect the anisotropic photoexcitation process. The peak position for the S $2p_{3/2} \rightarrow \pi^*$ excitation (hν=164.4 eV) corresponds to the lowest horizontal line in Fig. 1, where clear island-like structures are detected both in the horizontal and vertical directions in the kinetic energy region from 146 to 148 eV.

Figure 2 represents the enlargements of the resonant Auger spectra following the S $2p_{3/2} \rightarrow \pi^*$ excitation around the satellite region. The structures observed in the horizontal spectrum are good agreement with those in the previous work [1]. However, some differences are seen in the vertical spectrum; the peak position of the $^4\Pi$ state as labelled "0" in the horizontal spectrum differs from that in the vertical spectrum, and a peak at 17.8 eV is seen only in the vertical spectrum. Resonant Auger spectra with much higher resolution may reveal the reason for the discrepancy.

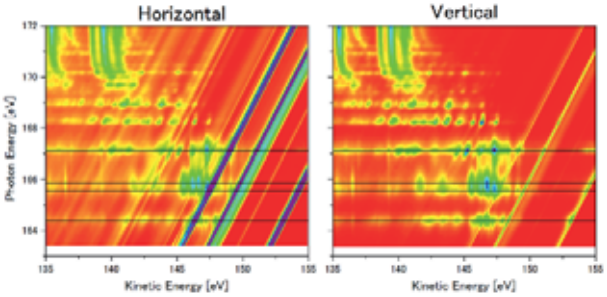

Fig. 1. 2D maps of resonant Auger electron spectra following the S 2p excitations of OCS, obtained at horizontal and vertical directions.

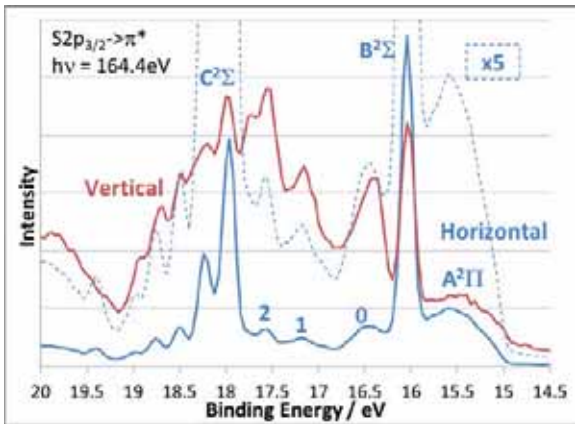

Fig. 2. Participator Auger spectra following the S $2p_{3/2} \rightarrow \pi^*$ excitation, measured at horizontal and vertical directions.

[1] S. Masuda, T. Hatsui and N. Kosugi, J. Electron Spectrosc. Rlat. Phenom. **137-140** (2004) 351.

Ultrafast Dynamics in C 1s Core-Excited CF_4 Studied by Two-Dimensional Resonant Auger Spectroscopy

M. N. Piancastelli[1], R. Guillemin[1], M. Simon[1], H. Iwayama[2] and E. Shigemasa[2]
[1]*LCPMR, Université Pierre et Marie Curie, 75231 Paris Cedex 05, France*
[2]*UVSOR Facility, Institute for Molecular Science, Okazaki 444-8585, Japan*

The CF_4 molecule, tetrafluoro methane, has been a benchmark for several spectroscopic studies, due to its high symmetry, same as methane, CH_4. One of the most interesting observations deriving from the comparison between CH_4 and CF_4 is the relative intensity of below-threshold photoabsorption structures around the C 1s ionization threshold associated with transitions to empty molecular orbitals versus Rydberg states. CF_4 is a good candidate to investigate the dynamical properties of core-excited states with an electron in the antibonding lowest-unoccupied molecular orbital (LUMO) in a highly symmetric system.

Here an investigation of ultrafast dissociation following C1s-to-LUMO core excitation in CF_4, with high-resolution resonant Auger spectroscopy, is presented. The main novelty of this work is the use of two-dimensional (2D) maps to record resonant Auger spectra across the resonance as a function of photon energy with a small energy step and then to characterize ultrafast dynamics. This method allows one to follow in great detail the evolution of the resonant enhancement of spectral features corresponding to final ionic states while scanning the energy across the resonance, and to fully exploit the so-called detuning effects.

The experiment was performed on the soft X-ray beamline BL6U at UVSOR. The photon energy resolutions were set to 10000 and 4000 for total-ion yield and 2D map measurements, respectively. Kinetic energies of the emitted electrons were measured by a hemispherical electron energy analyzer (MBS-A1). The direction of the electric vector was set to be parallel to the axis of the electrostatic lens of the analyzer. The kinetic energy resolution of the analyzer was set to 60 meV. The 2D maps were obtained by taking decay spectra at regular photon energy intervals of 100 meV across the resonance.

Figure 1 represents total ion yield curve measured in the C 1s excitation region of CF_4. The double feature with maxima at 297.7 and 298.4 eV is assigned to the Jahn-Teller-split transition to the LUMO (σ* of t_2 symmetry), followed by the Rydberg series. Figure 2 shows the 2D map after subtraction of the non-resonant contributions, and with on-top two pseudo-absorption curves obtained by the CIS (Constant Ionic State) method, and namely plotting the integrated intensity of the two resonant features, the non-dispersive one related to the fragment and the dispersive one related to the $3t_2$ state, as a function of photon energy. It is seen that while the intensity of the molecular state closely mimics one of the absorption curve, the non-dispersive feature related to the fragment decreases in relative intensity across the resonance, and disappears in the photon energy region of the Rydberg states. Detailed calculations on the potential curves of the intermediate and final state would be needed to fully clarify this finding.

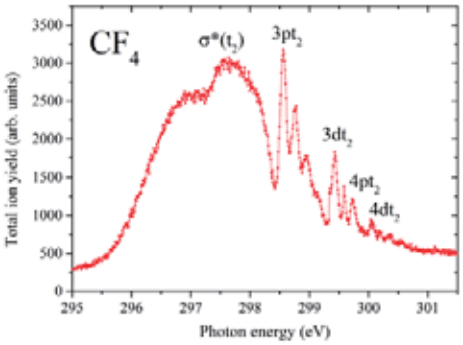

Fig. 1. Total ion yield curve measured in the C 1s excitation region of CF_4.

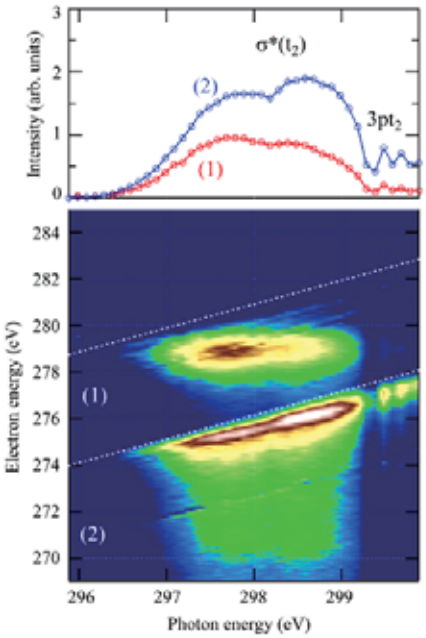

Fig. 2. Top: CIS spectra of the fragment (1) and of the $3t_2$ (2) final states. Bottom: resonant Auger 2-D map showing only the resonant contributions: (1) the non-dispersive state and (2) the $3t_2$ spectral line.

Cl-L_{23}VV Normal Auger and Resonant Auger Electron Spectra of CCl_4 Molecules

H. Iwayama[1], M. N. Piancastelli[2], R. Guillemin[2], M. Simon[2] and E. Shigemasa[1]
[1]*UVSOR Facility, Institute for Molecular Science, Okazaki 444-8585, Japan*
[2]*LCPMR, Université Pierre et Marie Curie, 75231 Paris Cedex 05, France*

The chlorofluoromethanes have received attention due to their potentially destructive effect on the earth's ozone layer. The inner-shell photoabsorption spectra of the family of tetrahedral molecules CX_4 (X=H, F, and Cl) are known to exhibit completely different below-threshold structures, related to transitions to empty molecular orbitals versus Rydberg states. The behaviors of the Rydberg state energies and intensities in these molecules are explained by the cage model, in which the Rydberg states are strongly excluded from CCl_4 but not from CF_4. CCl_4 has been a benchmark for several spectroscopic studies, due to its high symmetry, same as methane, CH_4, with four chlorine atoms around the carbon center. CCl_4 is one of the good candidates to investigate the dynamical properties of core-excited states with an electron in the antibonding unoccupied molecular orbitals in a highly symmetric system. We have studied the deexcitation processes following the Cl 2p excitations of CCl_4 molecules by using Auger electron spectroscopy.

The experiment was performed on the soft X-ray beamline BL6U at UVSOR. The radiation from an undulator was monochromatized by a variable included angle varied line-spacing plane grazing monochromator. The photon bandwidth was set to about 2000 (ΔE ~100 meV). Kinetic energies of the emitted electrons were measured by a hemispherical electron energy analyzer (MBS-A1). The direction of the electric vector was set to be parallel to the axis of the electrostatic lens of the analyzer. The kinetic energy resolution of the analyzer was set to 30 meV.

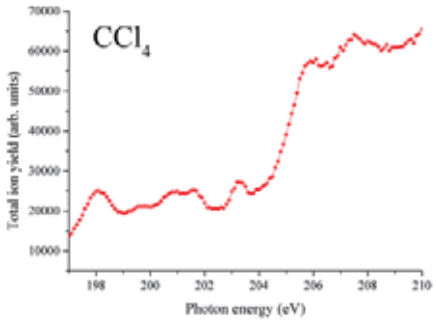

Fig. 1. Total ion yield curve in the Cl 2p excitation region of CCl_4.

Figure 1 shows the total-ion yield curve around the Cl 2p excitation region of CCl_4. The spectral features in Fig. 1 resemble the prevously measured high-resolution spectrum [1], where the photon bandwidth was about 30 meV. The broad peak around 198 eV is assigned to the excitation of the Cl $2p_{3/2}$ electron into the lowest unoccupied molecular orbital. The normal Auger electron spectrum and resonant Auger electron spectrum measured on top of this resonance are shown in Fig. 2. The present normal Auger spectrum displays clearer peak structures than that reported in Ref. [2], reflecting much higher resolution. Three peaks near 188 eV in the resonant Auger spectrum correspond to the photoionization of valence electrons. Two relatively sharp peaks around 180 eV seem to be strongly enhanced by the resonance. In order to examine the so-called detuning effect, higher photon energy resolution is required for measuring the resonant Auger spectrum, since its spectral resolution depends on the photon energy resolution. It is planned to record high-resolution resonant Auger spectra across the resonances as a function of photon energy.

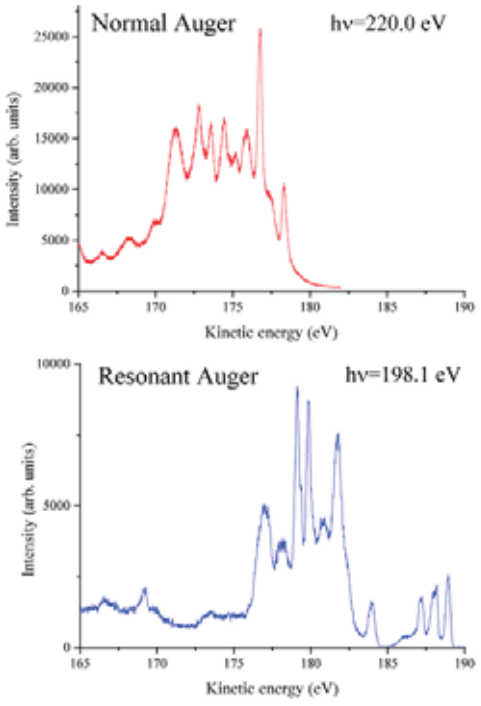

Fig. 2. Cl-L_{23}VV normal and resonant Auger spectra of CCl_4.

[1] M. de Simone *et al*., J. Phys. B **35** (2002) 61.
[2] P. G. Fournier *et al*., Phys. Rev. A **40** (1999) 163.

Ultrafast Molecular Dissociation of Core-Excited HCl Revisited

P. Lablanquie[1], F. Penent[1], H. Iwayama[2], K. Soejima[3] and E. Shigemasa[2]
[1]*LCPMR, Université Pierre et Marie Curie, 75231 Paris Cedex 05, France*
[2]*UVSOR Facility, Institute for Molecular Science, Okazaki 444-8585, Japan*
[3]*Department of Enviromental Science, Niigata University, Niigata 950-2181, Japan*

Excitation of a core electron to the lowest unoccupied antibonding orbital weakens the molecular bonding and populates generally a dissociative state. Morin and Nenner demonstrated that the 3d→σ* excitation in HBr leads to a fast neutral dissociation which can precede the Auger relaxation; in other words, one can observe 'atomic' 3d hole decays in the Br fragment [1].

In 2012 we showed that the equipment at UVSOR allows one to revisit the HBr fast dissociation with an unprecedented resolution, revealing more detailed atomic Auger peaks. Here we extend our studies and examine ultrafast dissociation following the Cl 2p core excitation in HCl.

The experiments were carried out on the soft X-ray beamline BL6U at UVSOR. The exit slit opening was set to 50 μm, which corresponds to a photon energy resolution ΔE of ~50 meV. The monochromatized radiation was introduced into a gas cell filled with sample gas. Kinetic energies of the emitted electrons were measured by a hemispherical electron energy analyzer (MBS-A1) placed at a right angle relative to the photon beam direction. The axis of the electrostatic lens of the analyzer was set to be parallel to the polarization direction of the incident light. The energy resolution of the analyzer was set to ~12 meV. Under these experimental conditions, the full width at half maximum of the vibrational fine structure for the A state of HCl^+ was measured to be ~65 meV.

Figure 1 (a) gives the resonant Auger spectrum measured on top of the $2p_{3/2} \rightarrow \sigma^*$ resonance. Comparison with the off resonance spectrum (b) shows that the molecular X, A and B HCl^+ states are little affected by the resonance, and reveals new peaks which are mainly the Atomic transitions:

$Cl\,(2p_{3/2})^{-1}\,3s^23p^6 \rightarrow Cl^+\,3s^23p^4$ or $Cl^+\,3s3p^5$

Broad structures at the foot of these peaks correspond to the 'molecular' autoionization during the HCl fast dissociation and amount to ~30% of the decays. The resonant spectrum can thus be used to retrieve the Auger spectrum associated with the decay of a 2p hole in a Cl atom. This is done in Fig. 2: (a) shows the decay of a $2p_{3/2}$ hole, as obtained on the $2p_{3/2} \rightarrow \sigma^*$ resonance, while (b) measured on the $2p_{1/2} \rightarrow \sigma^*$ resonance gives the decay of a $2p_{1/2}$ hole, with some contribution of the $2p_{3/2}$ hole decay. Comparison with the well-known Auger spectrum for the decay of a 2p hole in Ar in (c) is instructive as one can in this way compare the decay of a 2p hole in atoms with the same $3s^23p^6$ valence configuration, but with different nucleus. One observes a richer satellite structure for Cl (Fig. 2 (a) and (b)) compared to Ar (Fig. 2 (c)), which is probably linked to the difference of the 3d orbital in each case. Calculations are required to test this idea.

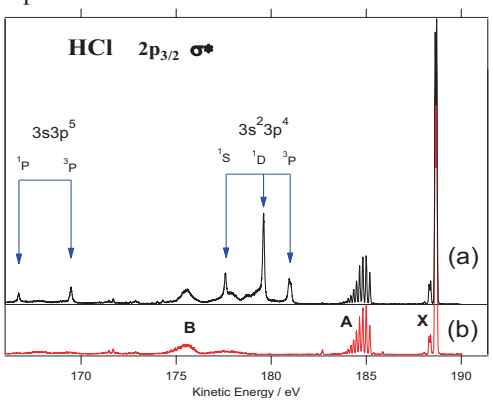

Fig. 1. (a) Resonant Auger spectrum measured on top of the $2p_{3/2} \rightarrow \sigma^*$ resonance, compared to a shifted off-resonance spectrum (b). Cl atomic lines are indicated with arrows.

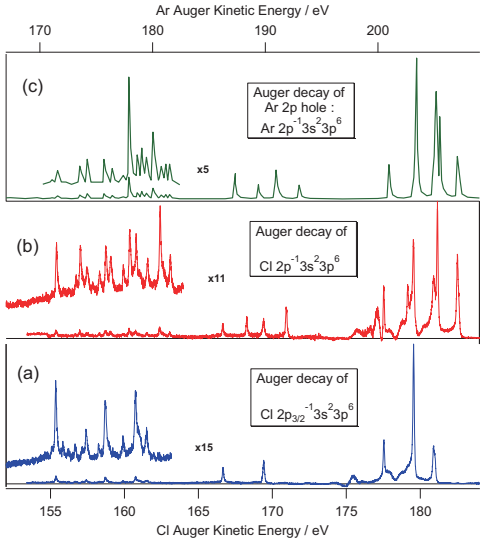

Fig. 2. Resonant Auger decay on $2p \rightarrow \sigma^*$ resonances showing the atomic Auger lines for the decay of $2p_{3/2}$ and $2p_{1/2}$ holes in Cl atoms ((a) and (b)), compared to the Auger spectrum for the decay of a 2p hole in Ar (from reference [2]).

[1] P. Morin and I. Nenner, Phys. Rev. Lett. **56** (1986) 1913.
[2] H. Pulkkinen *et al.*, J. Phys. B **29** (1996) 3033.

BL6U

Dissociation Pathways of Core Excited CF_4 Molecules Studied by an Auger-Electron–Ion Coincidence Method

H. Iwayama, L. Ishikawa and E. Shigemasa
UVSOR Facility, Institute for Molecular Science, Okazaki 444-8585, Japan

When a molecule composed of light elements is irradiated by soft x-rays, an inner-shell electron in the molecule is efficiently promoted into unoccupied molecular orbitals or continua. The core-hole state thus created is quite unstable, and subsequent Auger decay process follows in general. The molecular Auger final state possesses more than one hole in the valence orbitals, which often dissociates into two or more fragments. To understand such molecular photochemistry triggered by the core-hole creation, it is indispensable to correlate the Auger final states with the dissociation pathways. For this purpose, we have developed an Auger-electron-ion coincidence apparatus, which consists of a double toroidal electron analyzer (DTA) [1] and an ion momentum spectrometer. In the present work, we have studied dissociation pathways of core-excited CF_4 molecules around carbon K edge. In particular, we have investigated whether the dissociation processes following the core-to-Rydberg excitation differ from those after the core-to-valence excitation.

The Auger-electron-ion coincidence measurements for core-excited CF_4 molecules were carried out on the undulator beamline BL6U at UVSOR. The radiation from an undulator was monochromatized by a variable included angle varied line-spacing plane grazing monochromator. The electrons ejected at 54.7° with respect to the electric vector of the ionization light were analyzed in energy by DTA, while ions were extracted from the interaction region into the momentum spectrometer by a pulsed electric field according to the electron detection. Arrival positions on the detector and time-of-flights of ions were recorded for every event. The pass energy of the DTA was set to 200 eV for observing resonant Auger electrons. The energy resolution was about 1.9 eV. All signals from electron and ion detectors were recorded with an 8ch TDC board. We used photon energies of 298.5 and 299.4 eV, which correspond to C $1s\rightarrow\sigma^*(t_2)$ (valence) and $1s\rightarrow3pt_2$ (Rydberg) resonances, respectively [2]. The photon bandwidth was set to be 0.03 eV.

Figure 1 shows a resonant-Auger-electron–ion coincidence map obtained at the C $1s\rightarrow\sigma^*(t_2)$ resonance excitation. The vertical and horizontal axes of the map correspond to the kinetic energies of Auger electrons and the mass-to-charge ratios of ions, respectively. The one-dimensional spectra displayed in the right and top panels, represent the total events for the Auger electron detection and ion mass-to-charge rations, respectively. Main fragment ions were CF_n^+(n≤3) and F_n^+(n=1,2) ions. We didn't observe CF_4^+ parent ions within the present detection time. In the Auger-electron–ion coincidence map, we found that Auger electrons with high kinetic energy correlate with large fragment ions such as CF_2^+ and CF_3^+, while Auger electrons with low kinetic energy correlate with small fragment ions such as C^+ and F^+. This means that the Auger final states with high binding energy lead to efficient C-F bond breakings. The detailed data analyses are now in progress.

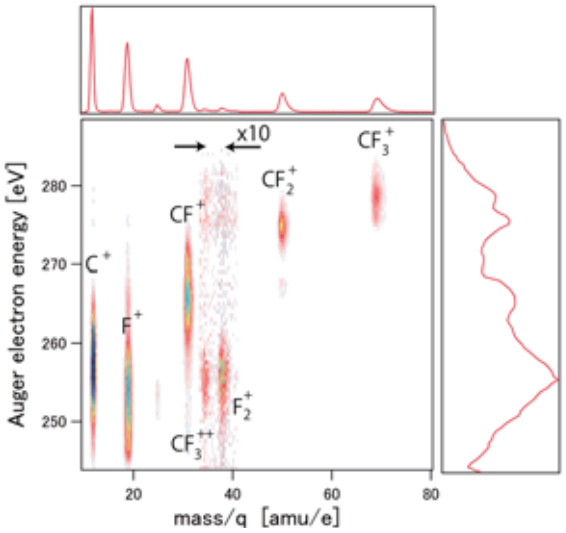

Fig. 1. Two-dimensional map for mass-to-charge ratios of ions in coincidence with resonant Auger electrons, obtained at the C $1s\rightarrow\sigma^*(t_2)$ resonance excitation of CF_4. The horizontal axis corresponds to mass-to-charge ratios of ions, and the vertical axis is the kinetic energies of the Auger electrons. The one-dimensional spectra shown at the right and top panels represent the total events for the Auger electron detection and the ion mass-to-charge ratios, respectively.

[1] C. Miron, M. Simon, N. Leclercq and P. Morin, Rev. Sci. Instrum. **68** (1997) 3728.
[2] R. Guillemin, W. C. Stolte, M.N. Piancastelli and D. W. Lindle, Phys. Rev. A **82** (2010) 043427.